Proceedings

A New Textile Economy: Synthesis and Characterization of Phenolic Type Resin with Protein from Waste Textiles Suitable for Wood-Based Panels †

Evangelia Tarani [1], Dimitra Patsiaoura [1], Electra Papadopoulou [2], Eleni Pavlidou [1], and Konstantinos Chrissafis [1,*]

[1] Laboratory of Advanced Materials & Devices, Physics Department, Aristotle University of Thessaloniki, GR 54124, Thessaloniki, Greece; etarani@physics.auth.gr (E.T.); dpatsi@physics.auth.gr (D.P.); elpavlid@auth.gr (E.P.); hrisafis@physics.auth.gr (K.C.)

[2] CHIMAR HELLAS S.A., 15 km National road Thessaloniki-Polygyros, P.O. Box 60666, GR 57001, Thessaloniki, Greece; Papadopoulou@ari.gr

* Correspondence: hrisafis@physics.auth.gr; Tel.: +30-2310-99-8188 (K.C.)

† Presented at the First International Conference on "Green" Polymer Materials 2020, 5–25 November 2020; Available online: https://cgpm2020.sciforum.net/.

Abstract: The population growth and the limited reservoir of fossil resources have ignited the attention of scientific communities and entrepreneurs to produce alternative products with raw-materials from renewable sources. In this work, proteins derived from the recycling of waste textiles were studied as raw-material in the synthesis of thermosetting polymers of a phenolic type suitable for use as adhesives in the production of wood-based panels. The chemical bonds between raw-materials and phenol-formaldehyde (PF) resins were verified with Fourier Transform Infrared spectroscopy. The curing performance and thermal stability of the thermosetting PF resins were studied with Differential Scanning Calorimetry and Thermogravimetric Analysis, respectively. Wood-based panels were prepared and tested at a lab scale following simulation of the industrial practice. Optical Microscope and Scanning Electron Microscopy were applied for the study of the interaction between PF resins and woodchips at the lab scale. It was found that the resins were successfully prepared. The maximum curing temperature of the experimental resins was shifted to higher values than the control PF. The protein-based resins seem to lose mass at a lower rate, which denotes that they are more thermally stable than a typical PF resin.

Keywords: PF resin; waste textiles; renewable sources; wood-based panels; curing; thermal stability

1. Introduction

In the woodworking industry, an essential application of adhesive is in manufacturing particleboards. The most used adhesives in the production of particleboards are the phenol formaldehyde (PF) and Urea-formaldehyde (UF) resins. PF resin presents some advantages such as fast curing, good performance in the panel, water solubility, and low price. PF resin is preferred by the wood-based panels industry due to its high reactivity and cost efficiency [1]. However, some disadvantages of PF is its dark color, expensive price, and formaldehyde emissions [2].

An ongoing effort is being made to enhance the properties of PF resin, and among others, to replace its petrochemical ingredients with renewable raw materials. Emphasis is placed on the replacement of formaldehyde by other chemicals of natural origin, or the reduction of formaldehyde emissions in PF-wood panels using bio-based additives [2,3]. Biomass belongs to the most promising candidates because it provides energy and a variety of chemical blocks appropriate for the synthesis

of many materials. Biomass from agricultural products or residues, animal wastes, textile wastes, is broadly available worldwide.

Global population growth has contributed to an increase in the production of textiles and, subsequently, textile waste. Textile wastes, when recycled, is a major source of natural and polymeric raw materials for the chemical and textile industry, as its main components are organic fibers (cotton (cellulose) and wool) and artificial fibers [3–6]. All these factors have attracted researchers to investigate the possibility of using textile wastes for the synthesis of adhesives.

In this study, an experimental PF resin with 20% phenol replacement by proteins derived from the recycling of waste textiles was studied and compared with a typical PF resin synthesized from petrochemical raw materials. The chemical bonds were verified with Fourier Transform Infrared spectroscopy (FTIR). The curing performance and thermal stability of the thermosetting PF resins were studied by using Differential Scanning Calorimetry (DSC) and Thermogravimetric Analysis (TGA), respectively. Wood-based panels were prepared and tested at a lab-scale following simulation of the industrial practice. For the study of the PF-woodchips interaction, Optical Microscope and Scanning Electron Microscopy (SEM) were applied. This project is a new idea of a circular economy to use waste fabrics as raw materials in the chemical and textile industry.

2. Materials & Methods

Both PF and PPF20 resins were kindly provided by the company CHIMAR HELLAS S.A. that produced them following a proprietary synthesis process suitable for industrial productions [7,8]. The experimental PF resin was synthesized by replacing 20% of the necessary phenol with proteins derived from the recycling of waste textiles (PFP20 sample name), while the typical PF resin was synthesized by using only petrochemical raw materials. Wood-based panels were prepared and tested at a lab-scale following simulation of the industrial practice.

FTIR in transmittance mode was used to study the synthesized materials. The spectra were received with a Spectrum 1000 Perkin-Elmer spectrometer in the spectral area 4000–400 cm^{-1}, a resolution of 2 cm^{-1} and 32 scans. For the resins in liquid form, the sandwich preparation method was used, in which a drop of hybrid is placed between two KBr pellets of 100 mg each. KBr pellets of 200 mg with 1 wt.% of the powdered material have been developed for solid samples.

TGA of the resins was carried out using a SETARAM SETSYS TG-DTA 16/18 instrument by heating the samples from 25 to 1000 °C in a 50 mL/min flow of air atmosphere at a heating rate of 20°C/min. Samples of 10 ± 0.5 mg were placed in alumina crucibles, while an empty alumina crucible was used as a reference.

DSC of the resins has been performed in a DSC 141 (Setaram). Temperature and energy calibrations of the instrument were performed for different heating rates, using the well-known melting temperature and melting enthalpies of high-purity Zinc, Tin, and Indium. The DSC measurements were carried out with liquid resin in stainless steel crucibles, while an identical empty crucible was used as a reference in each measurement. The samples were heated from ambient temperature to 250 °C with a heating rate of 5 °C/min in a 50 mL/min flow of nitrogen.

The samples were examined with a ZEISS STEMI DV4 microscope and their surface was photographed with a SONY Cybershot digital camera.

SEM micrographs of the prepared samples were studied by using a SEM JEOL JSM–390LV model. The specimens were carbon coated to provide good conductivity of the electron beam and the operating conditions were accelerating voltage 20 kV, probe current 45 nA, and counting time 60 s.

3. Results & Discussion

3.1. IR Analysis of PF Resins and PF/Woodchips Samples

Figure 1 shows the IR spectra of the typical PF resin, experimental PFP20 resin, woodchips, and the woodchips impregnated with synthesized resins. All spectra are characterized by the presence of a broad band of OH stretching in the 3300 cm^{-1} region. Bands of the typical PF and PFP20 resins at 1680–1650 cm^{-1}, 1480–1450 cm^{-1}, 1260 cm^{-1}, and 1060 cm^{-1} are assigned to C=O stretching of a benzene

ring, CH deformation in -CH$_2$ groups, biphenyl ether C-O stretching and dimethylene ether C-O deformation, respectively. The band observed at 1378 cm^{-1} is attributed to the in-plane deformation of phenolic OH. The bands at 1208 and 1225 cm^{-1} are attributed to the in-plane vibration of the C-O of the phenolic group. The bands at 1150 and 1050 cm^{-1} are characterized for the in-plane deformation of aromatic C–H [1].

The samples with woodchips, beyond the characteristic peaks of the resins, show the two bands of CH stretching at 2900 and 2800 cm^{-1}, and aromatic ring vibrations at the 1600–1500 cm^{-1}. The band at 1459 cm^{-1} is assigned to the C–H deformation in the –CH$_3$ of a methoxyl group. The band at 1380 cm^{-1} is attributed to C–O of a syringyl unit. The bands at 1170 cm^{-1} and 1042 cm^{-1} are assigned to the C–H stretching in a syringyl unit and the C–O of a primary alcohol, respectively [1].
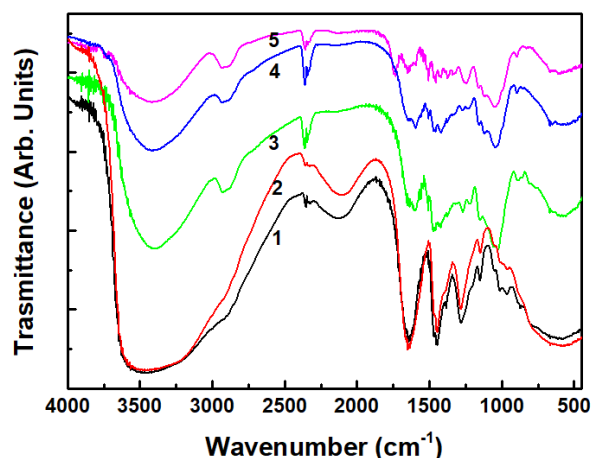

Figure 1. IR spectra of 1: PF, 2: PFP20, 3: PF/woodchips, 4: PFP20/woodchips, and 5: woodchips.

3.2. Thermal Study of PF Resins and PF/Woodchips Samples

Figures 2a and 2b show the TGA graphs and the corresponding derivative plot of the mass loss versus temperature (DTG) of the typical PF, PFP20 resin, PF/woodchips, and PFP20/woodchips samples. The TGA graph of the typical PF shows that degradation is completed in three steps. The first mass loss is performed at temperatures between 30 and 260 °C, where about 40% of the initial mass is lost due to the loss of water and small molecules like free formaldehyde and further crosslinking and loss of byproducts [7,9]. A further 10% of the mass is lost at the temperature range of 290–579 °C, where the pyrolytic degradation of polymers takes place. At 450 °C, the decomposition of aromatic rings takes place [10]. The DTG graph in Figure 2b shows the mass reductions by two endothermic curves at 136 °C and 465 °C. The above findings are consistent with literature references [7]. The TGA analysis of the PFP20 resin indicates an initial mass loss from 30 to 260 °C, which is attributed to the loss of the water content and emission of the unbounded formaldehyde in the resin. There is a mass loss of about 8% at 300–560 °C due to the breakdown of methylene linkages to produce aldehydes and phenols [7]. Finally, about 7.5% of the mass remains.

Woodchips were also subjected to TGA to investigate the decomposition and the highest temperature that can be safely applied during the production of the wood-based panels. The first mass reduction in the TGA plot is attributed to the water-humidity loss of the chips that occur close to 100 °C. The major mass loss of woodchips appears at 200–390 °C because of various organic compounds and wood degradation [7]. The TGA analysis of the PF/woodchips and PFP20/woodchips samples reveals a first mass loss up to the temperature of 170 °C. Above this temperature, the mass of the samples decreases. The mass degradation is ended at the same temperature for both resins. However, the PFP20/woodchips sample results in higher solid residue compared to PF/woodchips.
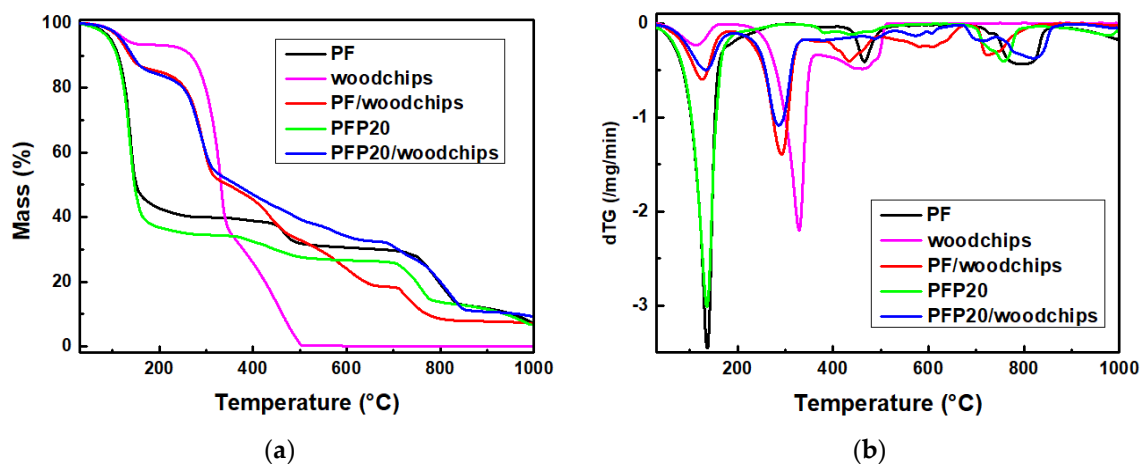
Figure 2. (**a**) Mass (%) and (**b**) DTG versus temperature of the typical PF, woodchips, PF/woodchips, PFP20 resin, and PFP20/woodchips.

The DSC thermographs of the typical PF, experimental PFP20 resin, PF/woodchips, and PFP20/woodchips are shown in Figure 3. The typical PF and the PFP20 resin exhibit an exothermic curve with a peak at the temperature of 145.5 and 159.8 °C, respectively. According to the literature [7], both peaks occur because of the reactions of chain building condensations. The PF/woodchips and PFP20/woodchips samples show similar exothermic curves but shifted to lower temperatures (109 and 113°C, respectively) compared to PF and PFP20 resins because of the ability of wood to accelerate the curing of the adhesives [7]. Nevertheless, the DSC graph of wood impregnated with PFP20 resin shows a significant reduction of peak temperature, the curing performance is still higher than that of the typical PF resin.
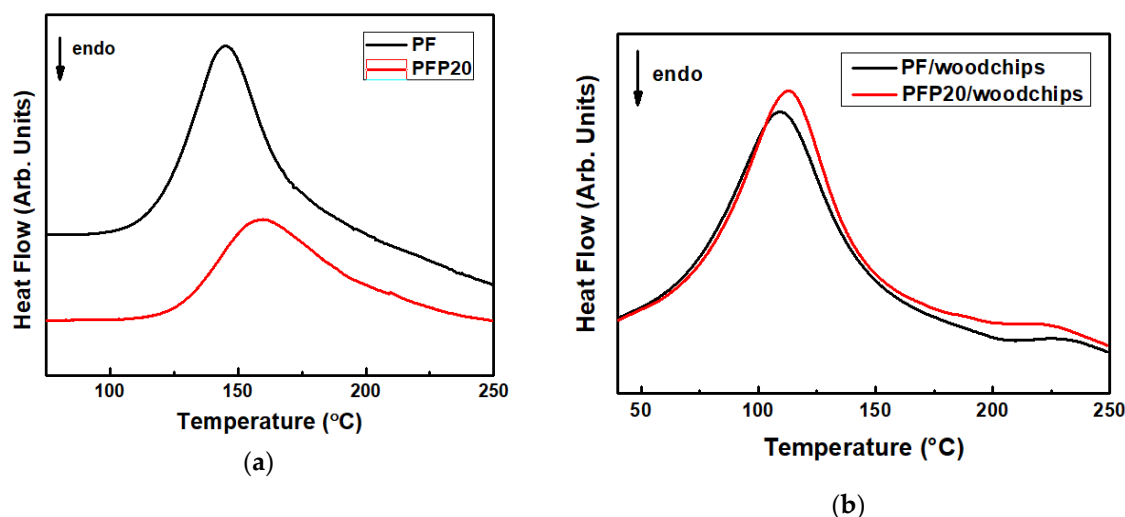

Figure 3. HeatFlow versus temperature of (**a**) typical PF and PFP20 resin and (**b**) PF/woodchips and PFP20/woodchips.

3.3. Morphological Characterization of PF/Woodchips Samples

Figures 4a-4f show the Optical Microscope Images of resin-wood composites (PF/woodchips and PFP20/woodchips). It was found that the woodchips are completely covered by the resins. However, the coverage is not uniform across its surface. Figures 4.a and 4.a show the resin-saturated regions and the formation of resinous deposits, whose presence has also been identified during SEM observation (see below). Figures 4c and 4d. show the cross-section Optical Microscope of PF/woodchips and PFP20/woodchips samples, respectively. The grinding process on the surface of the resin/wood composite was performed using sandpaper. It was impossible to estimate the

penetration depth of resins into the wood due to the limited resolution of the Optical Microscope. However, Figures 4c and 4d. confirm the resin's penetration into the wood structure, although many different fragments of wood and resin disrupt the Optical Microscope analysis.
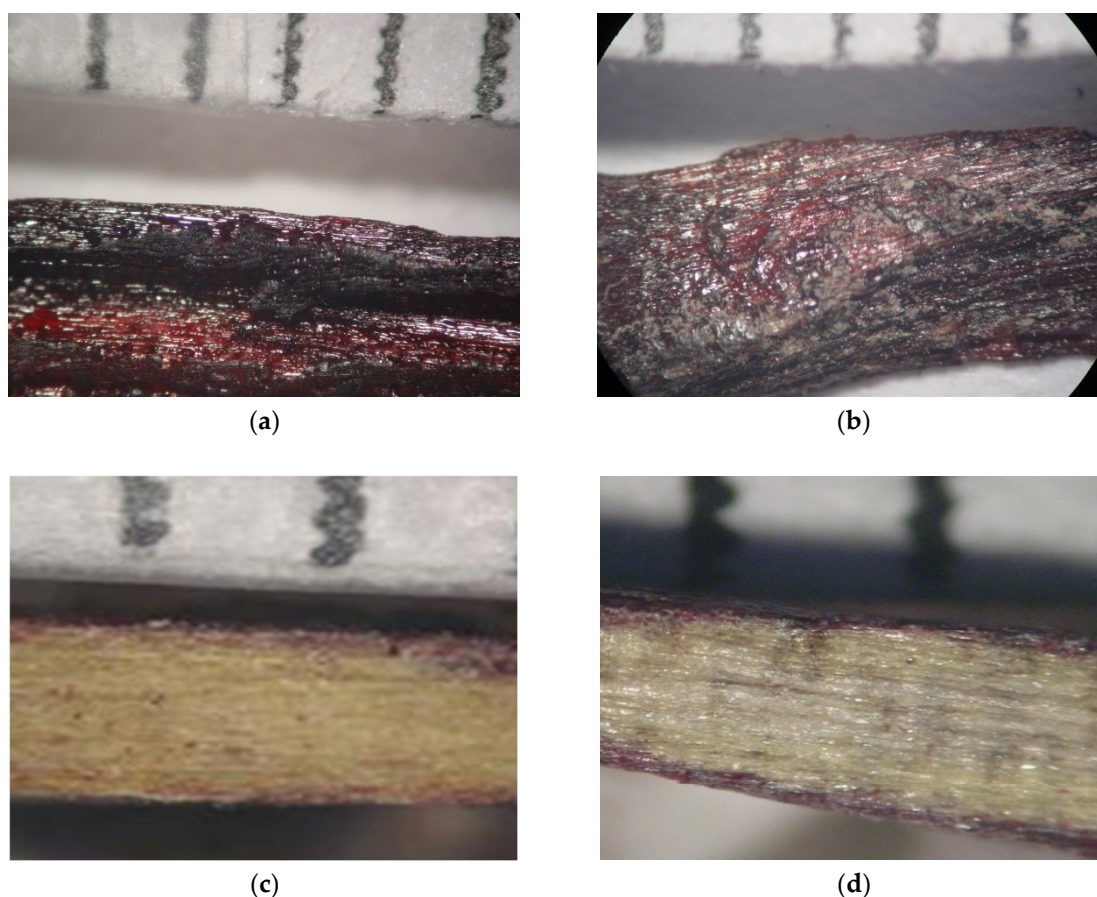

(**a**)

(**b**)

(**c**)

(**d**)

Figure 4. Optical Microscope images of (**a**), (**c**) control PF, and (**b**), (**d**) PFP20 resin.

Figures 5a-5d show the morphology of the resin/wood composites of the two resins used in this study (PF/woodchips and PFP20/woodchips). It was found that the woodchips are completely covered by the resins (SEM Images of PF/woodchips sample in Figures 5a, 5c, and SEM images of PFP20/woodchips sample in Figures 5b, 5d). So, the typical PF resin completely covers the wood without allowing any observation of the porous structure of the wood. On the contrary, the PFP20 resin allows the observation of the microstructure of the wood demonstrating the successful penetration of the resin on the wood surface.

Figures 6a-6c show the SEM Images of PFP20/woodchips sample obtained by grinding the surface of samples with sandpaper. As already mentioned, it is not possible to estimate the penetration depth of the resin into the woodchips due to the presence of many different fragments of resin and wood and to the organic nature of the two materials as well. Therefore, since the resin-wood distinction cannot be achieved, a comparative morphological study is performed between the two regions of the same sample. In Figure 6a, the middle area of the PFP20/woodchips composite in which the resin cannot penetrate is given in a yellow frame, while the green frame gives the area near the edges of the sample. The longitudinal lines running through the sample surface are due to the grinding process. Figures 6.b and 6.c show that the morphology of the two different points is different. Consequently, in the middle area (yellow), a "purer" sample morphology was observed compared to the edges of the PFP20/woodchips composite (green). This confirms the presence of the resin near the edges of the cross-sectioned sample. Also, in this case, the penetration depth of resin into the wood cannot be estimated.
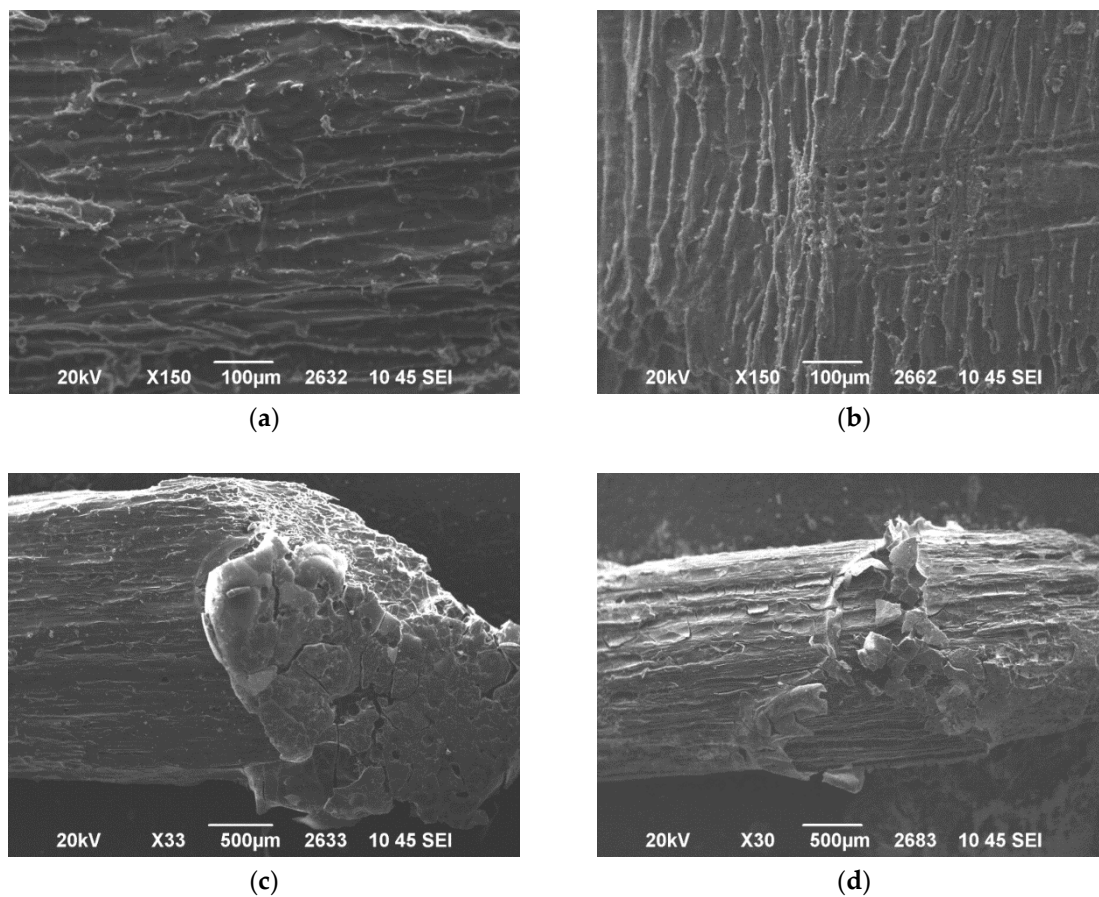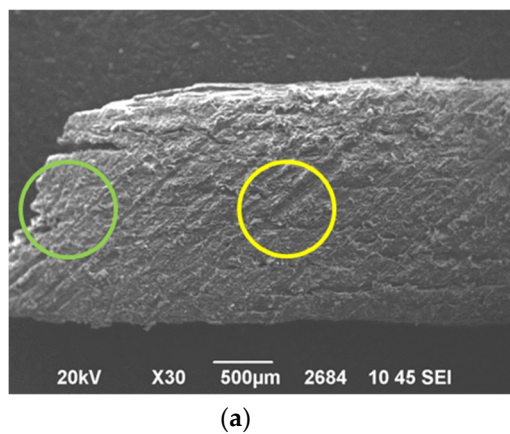
(**a**)

(**b**)

(**c**)

(**d**)

Figure 5. SEM images of (**a**), (**c**) typical PF, and (**b**), (**d**) PFP20 resin.

(**a**)

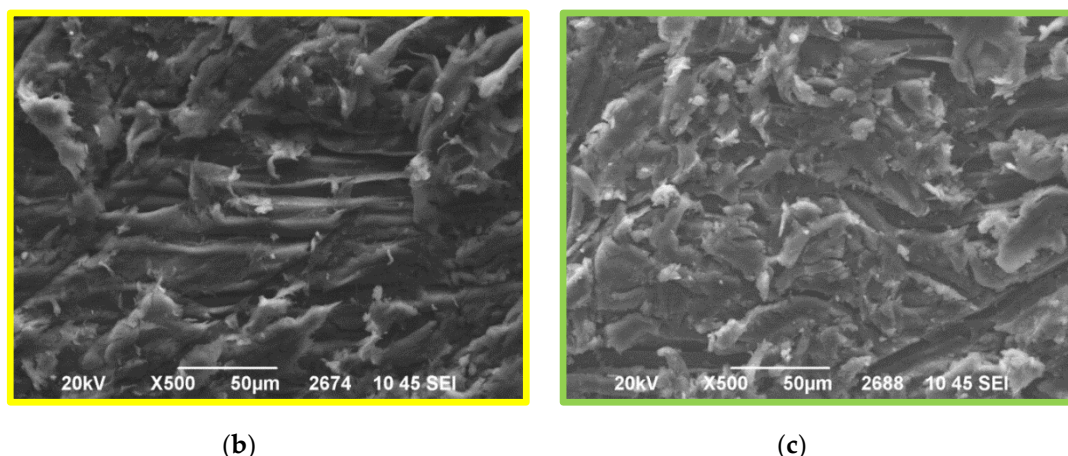|	
(**b**)	(**c**)

Figure 6. Cross-section SEM images of (**a**) PFP20/woodchips in (**b**) the middle (yellow) and (**c**) at the edge (green) of the sample.

4. Conclusions

In this work, the standard PF and PFP20 resins were found to have been prepared successfully. According to the IR analysis, the resins blended with woodchips, beyond the characteristic peaks of the resins, show peaks of the functional groups of woodchips. The mass degradation of the woodchips impregnated with resins is ended at the same temperature with the PFP20/woodchips sample to present higher solid residue compared to PF/woodchips. Additionally, although the PFP20 resin cures at a higher temperature than the typical PF resin, it has been shown that the PFP20/woodchips composite decreases the curing efficiency. Optical Microscope analysis and SEM micrographs confirm the resin's penetration into the wood structure with the PFP20 resin to allow the observation of the porous structure of the wood. We conclude that a PF resin with up to 20% phenol replacement by textile wastes can be considered competitive in the production of particleboards with a typical PF resin because it enables the partial replacement of phenol by a natural material supporting the sustainability of our ecosystem without coming behind in the performance and properties of the plywood panels.

Author Contributions: Conceptualization, K.C.; methodology, E.T, D.P. and E.S.P.; formal analysis, E.T and D.P.; investigation, E.T, D.P., and E.S.P.; writing—original draft preparation, E.T.; writing—review and editing, E.T, D.P., E.S.P., E.G.P., and K.C.; supervision, K.C.

Conflicts of Interest: The authors declare no conflict of interest.

Abbreviations

The following abbreviations are used in this manuscript:

PF: Phenol-Formaldehyde
PFP20: PF resin synthesized by replacing 20% of the phenol by proteins derived by textile wastes
UF: Urea-formaldehyde
DSC: Differential Scanning Calorimetry
TGA: Thermogravimetric Analysis
DTG: Derivative of mass
FTIR: Fourier Transform Infrared Spectroscopy
SEM: Scanning Electron Microscopy

References

1. Khan, M.A.; Ashraf, S.M.; Malhotra, V.P. Eucalyptus bark lignin substituted phenol formaldehyde adhesives: A study on optimization of reaction parameters and characterization. *J. Appl. Polym. Sci.* **2004**, *92*, 3514–3523.

2. Nemli, G.; Odabaş-Serin, Z.; Özdemir, F.; Ayrılmış, N. Textile dust for particleboard. *BioResources* **2019**, *14*, 120–127.

3. Zonatti, W.F.; Guimarães, B.M.G.; Duleba, W.; Ramos, J.B. Thermoset composites reinforced with recycled cotton textile residues. *Text. Cloth. Sustain.* **2015**, *1*, 1–12.

4. Temmink, R.; Baghaei, B.; Skrifvars, M. Development of biocomposites from denim waste and thermoset bio-resins for structural applications. *Compos. Part A Appl. Sci. Manuf.* **2018**, *106*, 59–69.

5. Wanassi, B.; Hariz, I. Ben; Ghimbeu, C.M.; Vaulot, C.; Jeguirim, M. Green carbon composite-derived polymer resin and waste cotton fibers for the removal of alizarin red S dye. *Energies* **2017**, *10*.

6. Qu, J.; Wang, Z.; Hu, C.; Yin, Q.; Pang, Y. Potential use of waste cotton in production of biomass composites. *BioResources* **2019**, *14*, 8424–8438.

7. Papadopoulou, E.; Chrissafis, K. Thermal study of phenol-formaldehyde resin modified with cashew nut shell liquid. *Thermochim. Acta* **2011**, *512*, 105–109.

8. Papadopoulou, E.; Kountouras, S.; Nikolaidou, Z.; Chrissafis, K.; Michailof, C.; Kalogiannis, K.; Lappas, A.A. Urea-formaldehyde (UF) resins prepared by means of the aqueous phase of the catalytic pyrolysis of European beech wood. COST Action FP1105. *Holzforschung* **2016**, *70*, 1139–1145.

9. Papadopoulou, E.; de Wild, P.J.; Kountouras, S.; Chrissafis, K. Evaluation of torrefaction condensates as phenol substitutes in the synthesis of phenol-formaldehyde adhesives suitable for plywood. *Thermochim. Acta* **2018**, *663*, 27–33.

10. Papadopoulou, E.; Kountouras, S.; Chrissafis, K.; Kirpluks, M.; Cabulis, U.; Švíglerová, P.; Benjelloun-Mlayah, B. Evaluation of the particle size of organosolv Lignin in the synthesis of resol resins for plywood and their performance on fire spreading. *Tappi J.* **2017**, *16*, 409–416.